Journal of Applied Polymer Science

Use of construction and demolition wastes as mineral fillers in hybrid wood–polymer composites

Anna Keskisaari, Svetlana Butylina, Timo Kärki
Department of Mechanical Engineering, Lappeenranta University of Technology, P.O. Box 20, Lappeenranta 53850, Finland
Correspondence to: A. Keskisaari (E-mail: anna.keskisaari@lut.fi)

ABSTRACT: The recycling of construction materials has been the subject of much research in past years. In this study, the use of construction and demolition wastes (CDWs) as mineral fillers in hybrid wood–polymer composites was studied. Two types of waste materials were used as fillers in the composites: (1) a mixture consisting of waste mineral wool (MW) and plasterboard (PB) and (2) mixed CDWs. The performance of the composites was evaluated from their mechanical properties and water-absorption behavior. We found in the study that the addition of mineral fillers decreased the flexural strength and modulus values of the wood–polypropylene (PP) composites. On the other hand, the exchange of part of the wood with a mineral filler resulted in an increase in the impact strength of the composite. The composite manufactured with the combination of MW and PB had the lowest water absorption. The decrease in wood loading resulted in improved dimensional stability in the hybrid wood–mineral filler–PP composites. © 2016 Wiley Periodicals, Inc. J. Appl. Polym. Sci. **2016**, *133*, 43412.

KEYWORDS: composites; fibers; recycling; thermoplastics

Received 8 September 2015; accepted 2 January 2016
DOI: 10.1002/app.43412

INTRODUCTION

The construction industry is a major solid-waste generator around the world.[1,2] Construction and demolition wastes (CDWs) include demolished concrete, bricks, and masonry, and wood and other materials, such as dry wall, glass, insulation, roofing, wire, pipe, rock, and soil.[3,4] The composition of CDW materials varies with the time and the place from which it has been collected.[5–8]

Because of the increased need for alternative solutions to disposal in landfills or controlled dumping sites, the recycling of both hazardous and nonhazardous wastes as secondary raw materials is becoming increasingly important. In accordance with the commitment of the European community, at least 79% of all CDWs must be prepared for reuse and recycling by 2020.[9] Recycling is one of the strategies in the minimization of waste, and it offers three benefits: it reduces the demand for new resources, cuts down transport and production energy costs, and allows the use of waste that would otherwise be lost to landfill sites.[10]

The possible and actual uses of recycled construction materials have been the subject of much research in recent years. For example, concrete aggregate has been extracted from many different concrete structures and recycled to produce new concrete with good technical and cost outcomes. The most common way to recycle concrete is to use it in the bound form (as an aggregate) to replace natural aggregates in new concrete and in the unbound form as a road base.[4] Waste-sourced gypsum [from plasterboard (PB)] may be used in stucco or plaster production and as a secondary component in cement production.[11] Mineral wool (MW) can be remelted into new wool, or it can be torn into loose wool and made into new insulation boards.[12] The recycling of rock wool in the concrete industry may be the most feasible application.[13]

Previous studies have shown that a combination of different fillers (e.g., wood fibers/flour and mineral fillers) in composites can be beneficial.[14,15] Hybrid composites combining two or more different types of fillers possess different properties that cannot be obtained with a single type of filler. In this study, the use of CDWs as mineral fillers in hybrid wood–polymer composites (WPCs) was studied. Two types of waste materials were used as fillers in the composites: (1) a mixture consisting of waste MW and PB and (2) mixed CDWs. The performance of the composites was evaluated from their mechanical properties and water-absorption behavior.

EXPERIMENTAL

Materials

The source of the wood fiber (WF) in the study was spruce (*Picea abies*) saw chips with a density of 1.58 g/cm^3. The saw chips were produced with a chipper combined with a hammer

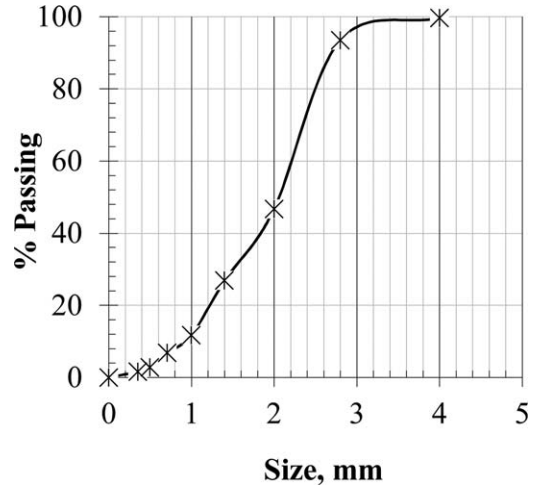

Figure 1. Particle size distribution of the wood material determined by sieve analysis.

mill. The chipper-blade protrusion was set to 2 mm. The size of the spruce particles and their distribution were measured with a set of sieves with a shaker (RETSCH Vibro 60480). The particle size distribution of the spruce particles is shown in Figure 1.

The thermoplastic matrix in the composite was commercially available polypropylene (PP) supplied by Ineos Polyolefins (Eltex P HY001P). The melt flow index of the PP was 45 g/10 min (230 °C), the melting point was 161 °C, and the density was 0.91 g/cm^3. The coupling agent was maleated polypropylene (MAPP), OREVAC CA 100 (Atofina, France). The Orevac CA 100 polymer had a low functionality (1%) and a high molar mass (25 kg/mol). Struktol TPW 113 was used as the lubricating agent.

Two types of waste materials were used as fillers in the composites: a 1:1 mixture of waste MW and PB (MW–PB) and mixed CDWs. All of the waste materials were obtained from a container containing CDWs at a local landfill. In the case of MW–PB, both the MW and PB were processed with a crusher and hammer mill apparatus (the same apparatus was used to treat

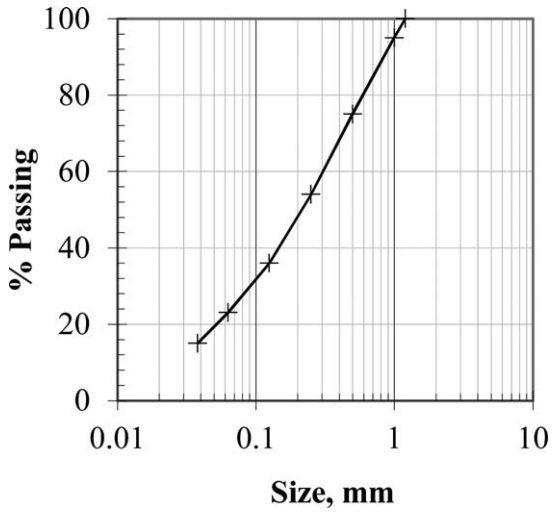

Figure 2. Particle size distribution of the burned CDW material determined by sieve analysis.

Figure 3. Ground CDW material used in the SEM–EDS analysis at magnifications of (a) 100 and (b) 500×.

the wood fibers) and mixed in a 1:1 ratio before the combination was used in the manufacturing of the composite. The mixed CDW material was burned at 800 °C and then sieved. The fraction, passed through a sieve with a mesh size of n16, was used to manufacture the composites. The particle size distribution of the burned waste is shown in Figure 2, and according to the Wentworth[16] classification, it consisted of sand, silt, and most likely, clay.

Analysis of the Mixed CDW Material

The aim of burning the CDW material was to get rid of organic contaminants. The temperature was around 800 °C. The treatment of mineral-containing samples at temperatures in the range 550–1100 °C in the so-called loss-on-ignition-test procedure is very often applied to minerals before analysis because it reduces the impurities in mineral-containing samples.[6,7,17,18]

The scanning electron microscopy (SEM)–energy-dispersive X-ray spectrometry (EDS) technique was used to study the chemical composition of the mixed CDW material. According to the recommendations for the preparation of mineral samples for analysis, the sample (25 g) was reduced to a powder with a size of 200–300 mesh by manual grinding in an agate mortar.[17] The loose powder (Figure 3) was used for energy-dispersive X-ray analysis. A JEOL JSM-5800 LV scanning electron microscope combined with Thermo a Noran System Six energy-dispersive X-ray spectrophotometer was used.

Table I. Chemical Composition of the Mixed CDW Material (Mass %)

Chemical composition	Mixed CDWs	Rock wool from basalt[19]	Slag wool melted in a cupola[19]
SiO	37.3	41–53	38–52
Al_2O_3	16.0	6–14	5–15
K_2O	3.5	0.5–2	0.3–2
Na_2O	3.6	1.1–3.5	0–1
MgO	1.9	6–16	4–14
CaO	20.8	10–25	20–43
TiO_2	0.7	0.9–3.5	0.3–1
FeO	3.0	3–8	0–2
SO_3	13.2	—	—

Figure 3 shows that the CDW material consisted of particles and fibers of different sizes and shapes. Because of the large amount of various particles, it was impossible to scan each particle separately. The average composition of the CDW material was determined after the analysis of 35 EDS spectra obtained for the area presented in Figure 3(a). Table I shows the average chemical composition of the mixed CDW samples, which were used to prepare the composites. A comparison of the average chemical composition of the burned CDW material with literature data available for MW[19] showed that the contents of the main oxides (e.g., SiO, Al_2O_3, and CaO) in the CDW material were in the range of values corresponding to rock/slag wool. MW is a generic term describing amorphous synthetic fibers produced from mineral raw materials, and it covers glass wool and rock/slag wool.[20] Similarities in the chemical compositions of the mixed CDW material and rock wool could be explained by the presence of fibers [visible in Figure 3(a, b)] and fused beads [Figure 4(a)], whose chemical compositions are like that of rock wool.

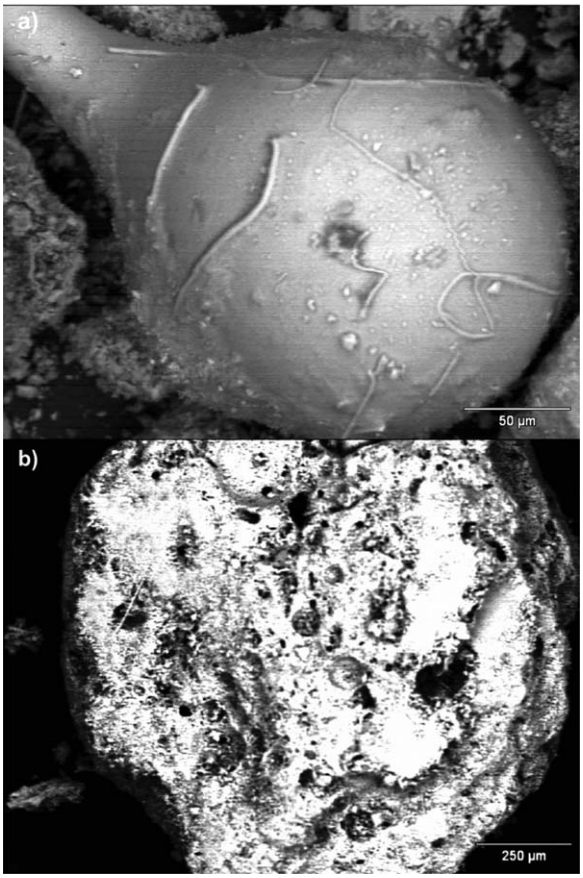

Figure 4. (a) Rock wool and (b) gypsum particles identified in the burned CDW material.

The main difference that distinguished the composition of the CDW material from rock/slag wool was the high content of sulfur oxide in the former (Table I). The peaks of sulfur in the EDS spectra of the mixed CDW material could be explained by the presence of gypsum particles [Figure 4(b)]. White porous particles, like the ones shown in Figure 4(b), were easily recognizable in the burned CDW material before it was ground. The SEM–EDS analysis of these white particles showed that they consisted of 50.6% SO_3 and 37.6% CaO; this was close to the literature data for gypsum, which had 52.7% SO_3 and 38.7% CaO.[21] As is known, gypsum loses all water of crystallization when it is heated to about 500 °C, and a porous anhydrite is formed.[22] According to the literature, the mineralogical composition of CDW includes tectosilicates, such as quartz and alkaline feldspars; micas, such as biotite and muscovite (granite rocks); calcite from the binder; illite; kaolinite; and gypsum.[3,6,7,23] Because of the lack of availability of an X-ray diffractometer, it was impossible to determine the precise mineralogical composition of the mixed CDW material used in this study.

Table II. Compositions of the Studied WPCs

Component	Composites (wt %)		
	WF–PP	WF–PP–MW–PB	WF–PP–CDW
Wood Fiber (WF)	64	24	44
PP	30	30	30
Coupling agent (MAPP)	3	3	3
Structol TPW113	3	3	3
MW	—	20	Identified
Gypsum from PB	—	20	Identified
Mixed CDWs	—	—	20

Processing

The compositions of the tested wood–mineral filler–PP composites are shown in Table II. All of the components were mixed together before extrusion with a TRL 100/FV/W turbomixer combined with an RFV-200 cooler (Plas Mec).

Hollow-shape decking boards (Figure 5) were produced with a Weber CE 7.2 conical twin-screw extruder (Hans Weber Maschinenfabrik GmbH, Kronach, Germany). The screw had a length-to-diameter ratio of 17, and the screw speed was 14 rpm. The barrel temperatures of the extruder were 170–190 °C. The melt temperature at the die was 176 °C. The pressure at the die varied between 2.5 and 3.0 MPa, depending on the material blend, and the material output was 25 kg/h.

Figure 5. Hollow profile of an extruded WPC with a width (W) of 126.0 mm and a height (H) of 20.0 mm.

Mechanical Properties

For the mechanical tests, 20 sample replicates were used. The flexural strength and modulus were determined according to standard EN 310 with a Zwick Roell (Z020) testing machine. The samples tested for the flexural properties had the following dimensions: length = 450 mm, width = 50 mm, and thickness of profile = 20 mm. A Charpy impact test on the unnotched rectangular test pieces was performed with a Zwick 5102 impact tester in accordance with the ISO 179/1-1fU standard. The test specimens for the Charpy impact test had the following dimensions: width = 10 ± 1 mm, thickness = 4 ± 1 mm, and length = 80 ± 1 mm. Also, they were cut from the extruded WPC panels.

SEM

SEM was performed with a JEOL JSM-5800 LV scanning microscope operating at 10 kV. Before analysis, the fractured surfaces were covered with a layer of gold with a sputter coater. Elemental analysis of the mineral-containing composites was performed with an energy-dispersive X-ray spectrometer.

Water Immersion Test

The resistance of the WPCs to water absorption was tested according to the procedure described in EN 317, which included 28 days of immersion of the WPCs in tap water. The tested samples had the following dimensions: length = 50 mm, width = 50 mm, and thickness of profile = 20 mm. The water absorption was determined as follows:

$$\text{Water absorption} = \left(\frac{m_t - m_0}{m_0}\right) \times 100 \quad (1)$$

where m_t is the mass of the sample after treatment (g) and m_0 is the mass of the sample before treatment (g).

The swelling in the thickness of the test samples was determined as follows:

$$\text{Thickness swelling} = \left(\frac{T_t - T_0}{T_0}\right) \times 100 \quad (2)$$

where T_t is the thickness of the sample after treatment (m) and T_0 is the thickness of the sample before treatment (m).

RESULTS AND DISCUSSION

Table III shows the mechanical properties of the composites. A two-sample t test was carried out with an α significance value of 0.05 in a comparison of the data of the reference WPC and the composites containing different mineral wastes. All statistical analyses were performed with Statgraphics Plus software (Version 4). As shown in Table III, the flexural strength and flexural modulus of the reference composite were significantly higher than the corresponding values of the composites containing waste mineral fillers. Comparative analysis of the flexural strength and flexural modulus values of the composites containing different mineral wastes showed that there was no statistically significance difference between them. Moreover, the flexural strength and flexural modulus of the composites containing waste were similar to the corresponding values obtained for a wood–PP composite made with recycled MW.[24] Studies of wood–MW hybrid composites prepared with intact MW[25] or recycled MW[24] have shown that the addition of MW results in a decrease in the flexural properties (the modulus of rigidity and modulus of elasticity) of the composites. Mamiński *et al.*[25] explained the decrease in the strength of composites after the addition of MW by the low cohesion of the wool domains with

Table III. Mechanical Properties of the Composites

Composite	Flexural strength (MPa)	Flexural modulus (GPa)	Charpy impact strength (kJ/m^2)
WF–PP	23.35 ± 0.56	4.44 ± 0.08	2.07 ± 0.13
WF–PP–MW–PB	18.75 ± 0.72[a]	3.83 ± 0.16[a]	2.34 ± 0.14[a]
WF–PP–CDW	17.79 ± 0.95[a]	4.04 ± 0.25[a]	3.09 ± 0.19[a]

[a] The difference between the reference composite and the composite containing waste was statistically significant at a p value of less than 0.05.

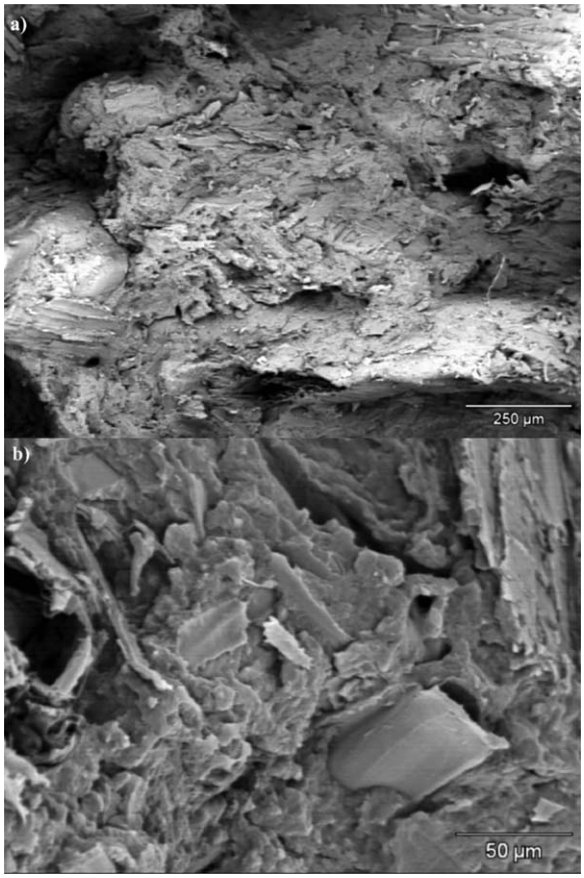

Figure 6. SEM micrographs of the WF–PP composite at magnifications of (a) 100 and (b) 500×.

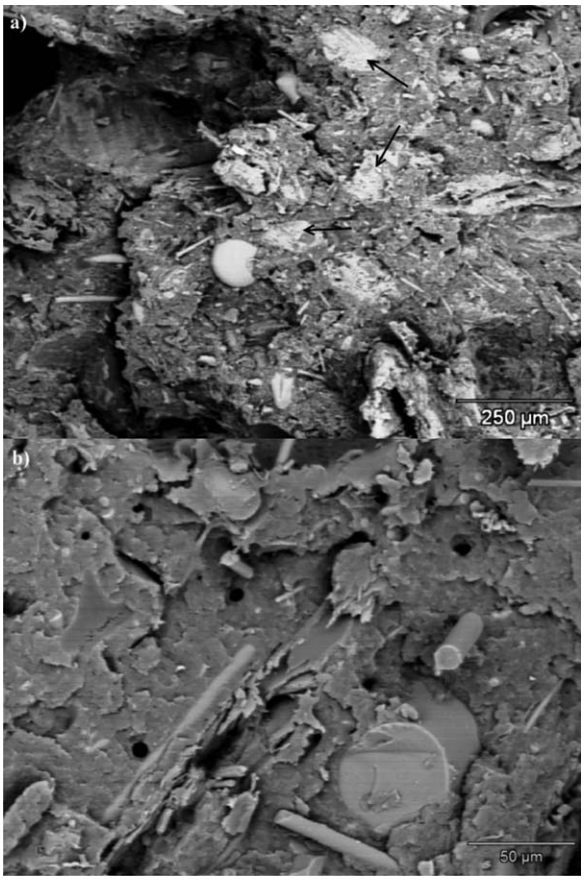

Figure 7. SEM micrographs of the WF–PP–MW–PB composites at magnifications of (a) 100 and (b) 500×.

the board, whereas according to Väntsi *et al.*,[24] the orientation of the MW fibers played an important role in the decrease in the flexural strength and modulus of the composites.

In their study on recycled MW, Väntsi *et al.*[24] found a 20% decrease in the flexural strength and a 14.9% decrease in modulus after the exchange of 20% wood fibers with recycled MW in a composite containing 64% filler and 30% PP. In this study, 19.7 and 23.8% decreases in the flexural strength and 13.7 and 9.0% decreases in the flexural modulus were evaluated for the WF–PP–MW–PB (containing 20% MW) and WF–PP–CDW composites, respectively, as compared to the reference composite. Therefore, we assumed that MW could have been one of factors affecting the decrease in the flexural properties of the WF–PP–MW–PB and WF–PP–CDW composites. The questions related to particle shape, size, orientation, and adhesion in the samples containing mixed waste material are addressed later in the section describing the SEM analysis of the fractured samples.

Table III also shows that in contrast to the decreased flexural strength and modulus, the values of the impact strength of the WPCs containing mineral waste were higher compared to those of the reference composite. The impact strength of the composites is a complex phenomenon that depends on the matrix properties, filler size, orientation, and adhesion between the fibers/particles and the matrix. The impact strength of WPCs is generally lower than the impact strength of pure PP (70 kJ/m^2).[26] The decreased impact strength of the WPCs in comparison with pure PP could be explained by the filler properties. Fillers can act as stress concentration points. They can also reduce the mobility of the polymer chain and, thereby, reduce the ability to absorb energy during fracture propagation. These two mechanisms of energy reduction are common for all fillers. In the case of WPCs with a high content of wood loading, the agglomeration of wood fibers is a very often occurring phenomenon. The agglomeration of wood fibers can initiate crack formation and, thus, decrease the energy required. Therefore, the higher impact strength of the WPCs

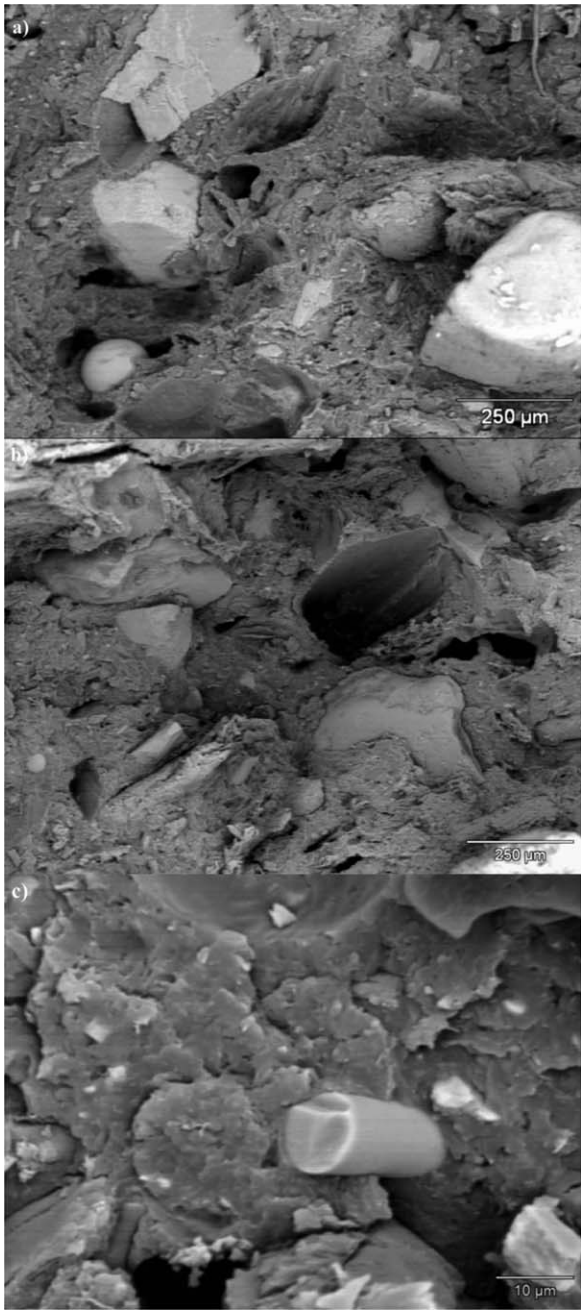

Figure 8. SEM micrographs of the WF–PP–CDW composite at magnifications of (a,b) 100 and (c) 1000×.

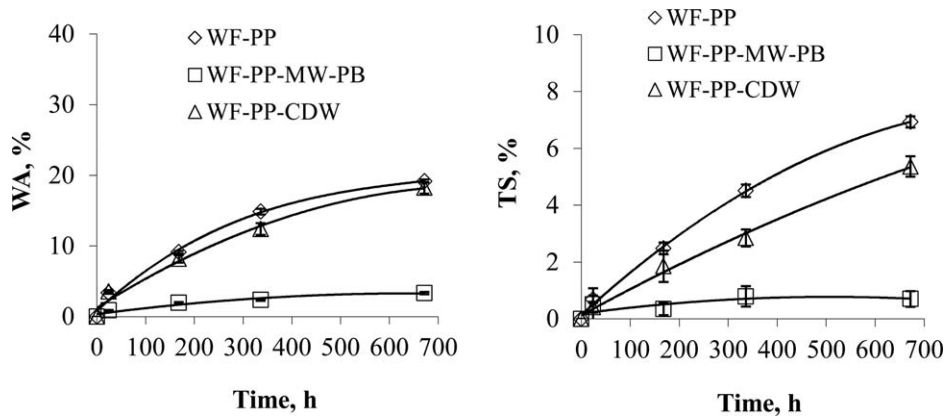

Figure 9. (a) Water absorption (WA) and (b) thickness swelling (TS) of the composites as a function of the time.

containing mineral waste could be explained by the lower content of wood fibers in them compared to that in the reference composite.

SEM–EDS Analysis

Figures 6–8 show SEM images of the fractured surfaces of the composites. In the reference composite, the polymer matrix was filled with wood fibers. The fiber aggregates and large wood particles, which could be seen on the fractured surface of the reference composite [Figure 6(a)], were pulled out from the matrix and left large cavities. The breakage of wood fibers [Figure 6(b)] was also found on the fractured surface of the reference composite. It should be noted that the wood fibers and large wood particles were oriented randomly, and the polymer martix had a large number of openings (porosity).

The loading of wood in the WF–PP–MW–PB composite was 2.7 times lower than that of the reference composite. In the case of the WF–PP–MW–PB composite, the lower wood loading in the polymer matrix resulted in the improved distribution of wood fibers and decreased the amount of wood aggregates.

SEM–EDS analysis confirmed that the cylindrical fibers and fused beads that could be seen on the fractured surface of the WF–PP–MW–PB composite [Figure 7(a)] belonged to MW. The diameters of the MW fibers varied [Figure 7(b)], and the smallest MW fibers were capable of effectively filling the pores in the composite structure. The MW fibers had a random orientation. The SEM analysis showed that the fractured surface of the WF–PP–MW–PB composite had a large number of openings left from MW fiber pullouts. By means of the SEM–EDS analysis, the white spots, marked with arrows in Figure 7(a), on the fractured surface of the WF–PP–MW–PB composite, were identified as gypsum.

Fused beads and fibers similar to those found in the WF–PP–MW–PB composite were also detected on the fractured surface of WF–PP–CDW (Figure 8). Comparison of their chemical composition with the composition of MW from the WF–PP–MW–PB composite by SEM–EDS showed that they were identical. The fractured surfaces of the WF–PP–CDW composite were characterized by the presence of mineral particles with different shapes and sizes and also varied chemical composition. The SEM–EDS analysis revealed that most of the mineral particles had an aluminosilicate nature (feldspars), a few particles were identified as silicon dioxide (sand), and small inclusions of iron were detected on the surface of some mineral particles. The presence of openings of different shapes, similar to the shapes of mineral particles, in the matrix of the WF–PP–CDW composite indicated that the pullout of mineral particles was a dominating fracture mechanism.

The porosity of the matrix of the WF–PP–CDW composite was similar to that of the reference composite. In contrast to the WF–PP–MW–PB composite, no white spots associated with gypsum were found on the fractured surface of this composite. The lack of detectable gypsum spots could be explained by the lower concentration of gypsum in the initial composition of the WF–PP–CDW composite compared to that of the WF–PP–MW–PB composite.

Water-Absorption Behavior of the Composites

The results of the water-absorption tests are shown in Figure 9. The water absorption of the reference and the WF–PP–CDW composite was similar and much higher than the water absorption of the WF–PP–MW–PB composite. Pure PP was hyrdophobic and was unable to absorb water, and the fillers were believed to be the main reason for the absorption of water by the composites. Wood fibers have free hydroxyl groups in cellulose and hemicellulose; these represent the sites for water absorption. It was expected that the reduction of wood loading in the WF–PP–MW–PB and WF–PP–CDW composites would decrease their water absorption compared to the reference composite. The porosity of the matrix of composites also affected their water absorption. The lowest water absorption of the WF–PP–MW–PB composite could be explained by the low content of wood, and the pore-filling effect of MW fibers revealed by SEM.

Similar to the water-absorption curves, the thickness swelling of the composites increased with time. A strong correlation was found between the loading of wood fibers and the thickness swelling of the composite (correlation coefficient = 0.96). This could be explained by the fact that with all of the added fillers, the dimensions of wood changed most easily in swelling. Therefore, exchanging part of the wood fibers with mineral waste materials would improve the dimensional stability of the composites.

CONCLUSIONS

In this study, hybrid wood–mineral waste PP composites were manufactured by extrusion, and their mechanical properties and water-absorption properties were studied. The exchange of part of the wood with waste mineral fillers resulted in decreases in the flexural strength and modulus but an increase in the impact strength of the composites. The water absorption and thickness swelling of the composites depended on the wood loading. The exchange of wood fibers with waste mineral fillers improved the water-absorption behavior of the composites. This study demonstrated that mineral wastes can be used as fillers in hybrid composites. However, thorough analysis and separation/purification of waste components is required, as some components can have adverse effects on the properties of the composites.

REFERENCES

1. European Environmental Agency. The European Environment—State and Outlook 2010: Synthesis; European Environmental Agency: Copenhagen, **2010**.
2. Poon, C. S.; Yu, A. T. W.; Ng, L. H. *Resour. Conserv. Recycl.* **2001**, *32*, 157.
3. Bianchini, G.; Marrocchino, E.; Tassinari, R.; Vaccaro, C. *Waste Manage.* **2005**, *25*, 149.
4. Tam, V. W. Y.; Tam, C. M. *Resour. Conserv. Recycl.* **2006**, *47*, 209.
5. Gualtieri, A. F.; Giacobbe, C.; Sardisco, L.; Saraceno, M.; Lassinatti Gualtieri, M.; Lusvardi, G.; Cavenati, C.; Zanatto, I. *Waste Manage.* **2011**, *31*, 91.
6. Angulo, S. C.; Ulsen, C.; John, V. M.; Kahn, H.; Cincotto, M. A. *Waste Manage.* **2009**, *29*, 721.
7. Limbachiya, M. C.; Marrocchino, E.; Koulouris, A. *Waste Manage.* **2007**, *27*, 201.
8. Wahlström, M.; Laine-Ylijoki, J.; Määttänen, A.; Luotojärvi, T.; Kivekäs, L. *Waste Manage.* **2000**, *20*, 225.
9. Directive 2008/98/EC of the European Parliament and of the Council, 19 November **2008**, on Waste and Repealing Certain Directives. Official Journal of the European Union 2008; L 312/3.
10. Edwards, B. Sustainable Architecture: European Directives and Building Design, 2nd ed.; Architectural: Oxford, United Kingdom, **1999**.
11. Coelho, A.; de Brito, J. *J. Clean Prod.* **2013**, *39*, 338.
12. Thormark, C. *Resour. Conserv. Recycl.* **2001**, *33*, 113.
13. Cheng, A.; Lin, W-T.; Huang, R. *Mater. Des.* **2011**. *32*, 636.
14. Nurdina, A. K.; Mariatti, M.; Samayamutthirian, P. *J. Vinyl Addit. Technol.* **2009**, *15*, 20.
15. Huuhilo, T.; Martikka, O.; Butylina, S.; Kärki, T. *Baltic For.* **2010**, *16*, 126.
16. Wentworth, C. K. *J. Geol.* **1922**, *30*, 377.
17. Johnson, W. M.; Maxwell, J. A. Rock and Mineral Analysis, 2nd ed.; Wiley: New York, **1981**; p 55.
18. Sun, H.; Nelson, M.; Chen, F.; Husch, J. *Can. J. Soil Sci.* **2009**, *89*, 603.
19. Agency for Toxic Substances and Disease Registry. Toxicological Profile for Synthetic Vitreous Fibers; U.S. Department of Health and Human Services: Atlanta, **2004**.
20. Müller, A.; Leydolph, B.; Stanelle, K. *Interceram* **2009**, *58*, 378.
21. Carvalho, M. A.; Junior, C. C.; Junior, H. S.; Tubino, R.; Carvalho, M. T. *Mater. Res.* **2008**, *11*, 391.
22. Withington, C. F.; Jaster, M. C. Selected Annotated Bibliography of Gypsum and Anhydrite in the United States and Puerto Rico; U.S. Government Printing Office: Washington, DC, **1960**; p 4.
23. Rodrigues, F.; Carvalho, M. T.; Evangelista, L.; de Brito, J. *J. Clean Prod.* **2013**, *52*, 438.
24. Väntsi, O.; Kärki, T. *Constr. Build. Mater.* **2014**, *55*, 220.
25. Mamiński, M. Ł.; Król, M. E.; Jaskółowski, W.; Borysiuk, P. *Eur. J. Wood Wood Prod.* **2011**, *69*, 337.
26. Nygård, P.; Tanem, B. S.; Karlsen, T.; Brachet, P.; Leinsvang, B. *Compos. Sci. Technol.* **2008**, *68*, 3418.